DOI: http://dx.doi.org/10.12989/sem.2007.27.6.697

An applied model for steel reinforced concrete columns

Xilin Lu† and Ying Zhou‡

State Key Laboratory for Disaster Reduction in Civil Engineering, Tongji University, Shanghai, 200092, P. R. China

(Received March 16, 2005, Accepted October 30, 2007)

Abstract. Though extensive research has been carried out for the ultimate strength of steel reinforced concrete (SRC) members under static and cyclic load, there was only limited information on the applied analysis models. Modeling of the inelastic response of SRC members can be accomplished by using a microcosmic model. However, generally used microcosmic model, which usually contains a group of parameters, is too complicated to apply in the nonlinear structural computation for large whole buildings. The intent of this paper is to develop an effective modeling approach for the reliable prediction of the inelastic response of SRC columns. Firstly, five SRC columns were tested under cyclic static load and constant axial force. Based on the experimental results, normalized trilinear skeleton curves were then put forward. Theoretical equation of normalizing point (ultimate strength point) was built up according to the load-bearing mechanism of RC columns and verified by the 5 specimens in this test and 14 SRC columns from parallel tests. Since no obvious strength deterioration and pinch effect were observed from the load-displacement curve, hysteresis rule considering only stiffness degradation was proposed through regression analysis. Compared with the experimental results, the applied analysis model is so reasonable to capture the overall cyclic response of SRC columns that it can be easily used in both static and dynamic analysis of the whole SRC structural systems.

Keywords: steel reinforced concrete (SRC); applied model; ultimate bearing strength; skeleton curve; hysteresis rule.

1. Introduction

Steel reinforced concrete (SRC) structure is usually called composite steel-concrete strucrture. One important advantage of SRC systems is that construction is accelerated through separation of working procedures. Initially, a bare steel frame is erected to carry the gravity, construction, and lateral loads during construction. As erection of building processes, concrete is cast in lower-level columns to form the composite system that will resist the total gravity and lateral loads. The development of the hybrid construction is the result of pursuing the economical, high-efficiency of the construction. Structural engineers also expect to obtain the following merits by employing the SRC structural systems: increase of stiffness, strength, ductility and fire resistance capacity; reduction of amount of steel; and smaller cross-section of high-rise and long-span framing systems

† Professor, Vice Director, Corresponding author, E-mail: lxlst@mail.tongji.edu.cn
‡ Ph.D., Lecturer, E-mail: yingzhou@mail.tongji.edu.cn.

(Morino 1997). Accordingly, SRC frame or frame-wall structures are effective for resisting lateral loads imposed by wind or earthquakes. These systems provide substantial lateral strength and stiffness as well as the inelastic deformation capacity needed to meet the demand of the earthquake ground motions. In order to predict the inelastic response of such structural systems under seismic loads, the hysteretic behavior of the structural members and their interaction should be described by reliable analytical models.

Constitutive member models are required for both structural design and seismic evaluation of building systems. In recent years, the emphasis of structural design for seismic resistance has been changing from “strength” to “performance”. In the performance-based design, analytical member models have to be introduced to the pushover and time-history analysis to achieve the seismic response of the structures. To save the computation time, constitutive models on the basis of members are more effective to the seismic evaluation of the whole building systems.

Relative simplicity and reasonable accuracy are emphasized as prerequisites of a member model for use in design and evaluation of structural systems. Analytical modeling of the inelastic response of SRC members can be accomplished by using either a microcosmic finite element model based on a detailed interpretation of the local behavior, or by using a macroscopic model based on capturing overall behavior with reasonable accuracy. Although the finite element method provides a powerful tool, due to the lack of completely reliable models and the complexities involved in the analysis and interpretation, difficulties may arise in the implementation and interpretation of the microcosmic models. Macroscopic models, on the other hand, are based on a simplified idealization and are confirmed to be valid for use both in static and dynamic analysis of complex building structures. In the macroscopic model, parameters are introduced to represent the stiffness degradation, strength deterioration and pinching effect of members, e.g. the three-parameter model (Park *et al.* 1987). Reasonable member models with typical parameters would be the best timesaving choice for the structural analysis to reflect the inelastic deformation features.

By now, although extensive research has been carried out for the ultimate strength of SRC members under static and cyclic load, there was only limited information on the analytical models (Ricles and Paboojian 1994, El-Tawil and Deierlein 1999, Deierlein and Noguchi 2004, Aschheim 2000, Geol 2004). The physical phenomena underlying the response of the model to quasi-static and dynamic loading have not been rigorously studied and the model has not been calibrated with reliable experimental data.

Given these shortcomings, five SRC column specimens were tested under cyclic lateral load and constant axial force in this paper to calibrate the model for SRC columns. After analyzing the experimental response and load-displacement curves of the specimens, simplified trilinear skeleton curve were put forward in term of the normalization of ultimate bearing strength. Theoretical equation of controlling point (ultimate strength point) was built up on the basis of load-bearing mechanism of RC columns and verified by the 5 specimens in this test and 14 SRC columns from parallel tests. Since no obvious strength deterioration and pinch effect were observed in the experimental load-displacement curves, hysteresis rule considering only stiffness degradation was proposed through regression analysis. Compared with the experimental results, the simplified analytical model is so reasonable to capture the overall cyclic response of SRC columns that it can be easily applied in both static and dynamic structural analysis.

2. Test on SRC columns

2.1 Test specimens

Five SRC column specimens were tested to assess and calibrate the model. The testing columns had a total length of 1820mm with a crisscross joint in the middle representing the connection between columns and beams. The columns R1, R2, R3 of the five specimens had a rectangular section with dimensions of 150 mm × 300 mm and the other two columns S1, S2 had a square section with dimensions of 150 mm × 150 mm. The reinforcement of all five columns consisted of 4

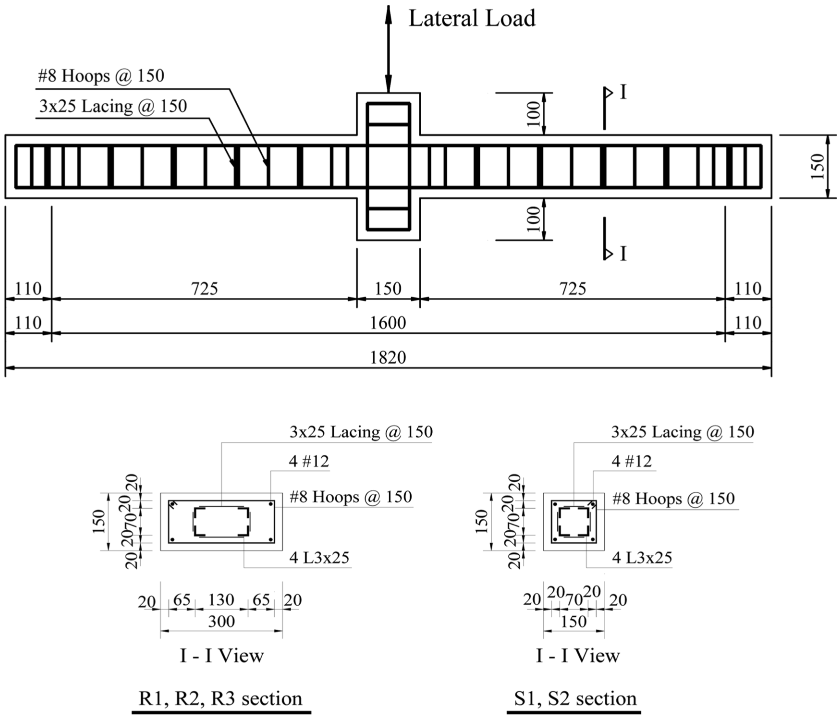

Fig. 1 Details of the specimens (units: mm)

Table 1 Reinforcement details of specimens

Specimen name	Section		Reinforcement		Longitudinal steel ratio (%)	Axial load		Section configuration
	Width (mm)	Height (mm)	Longitudinal	Transverse		Force (kN)	Axial force ratio n_0	
R1	301	154	4#12 4 L3 × 25	#8 @ 150 mm 3 × 25 @ 150 mm	1.0% 1.3%	496.4	0.69	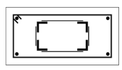
R2	300	150	4#12 4 L3 × 25	#8 @ 150 mm 3 × 25 @ 150 mm	1.0% 1.3%	376.3	0.54	
R3	300	151	4#12 4 L3 × 25	#8 @ 150 mm 3 × 25 @ 150 mm	1.0% 1.3%	188.2	0.27	
S1	150	150	4#12 4 L3 × 25	#8 @ 150 mm 3 × 25 @ 150 mm	2.0% 2.5%	250.9	0.73	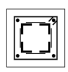
S2	150	150	4#12 4 L3 × 25	#8 @ 150 mm 3 × 25 @ 150 mm	2.0% 2.5%	188.2	0.55	

Note: The axial ratio n_0 is defined as the ratio of the longitudinal force N to the axial load bearing capacity of the concrete $f_c bh_0$, in which h_0 represent the effective height of the section.

Table 2 Experimental material properties

Specimen	Nominal yield strength (MPa)	Yield strength (MPa)	Ultimate strength (MPa)
Rebar, #8	210	235.0	355.0
Rebar, #12	310	351.0	507.3
Angle steel, L3x25	–	262.6	262.6
Concrete	–	–	20.1/19.0

#12 longitudinal bars (nominal bar diameter 12 mm) and 4 L3 mm × 25 mm angle steels (leg length 25 mm). They were tied together by #8 seismic hoops and by 3 mm × 25 mm lacings along the length. The clear cover to the stirrup was 20 mm. Details of the five specimens are shown in Fig. 1 and tabulated in Table 1.

2.2 Material properties

The material properties are summarized in Table 2. The material of steel was Grade II with a nominal yield stress of 310 MPa for longitudinal rebar, and 210 MPa for angle steels. The actual yield strength and ultimate strength are summarized in Table 2. Normal-strength concrete was used in the specimens. The concrete cubic compressive average strength was tested to be 20.1 MPa for R1, R2, R3 specimens and 19.0 MPa for S1, S2 specimens, using 15 cubic specimens with a dimension of 150 mm × 150 mm × 150 mm.

2.3 Instrumentation

The applied horizontal (axial) forces were measured using calibrated load cells with a range of 600 kN, and the vertical displacements were recorded using linear potentiometers. Electrical resistance strain gauges were used to measure the strains of the steel angle and reinforcing bars at selected locations in the SRC specimen. Note that in the post-test data analysis, the actual vertical mid-span displacements of the specimens were obtained by subtracting the support deformations from them.

2.4 Test setup

The test setup is shown in Fig. 2. A constant axial load was applied by a horizontal actuator, which was force controlled, so that a constant axial force was maintained throughout the testing. Lateral quasi-static cyclic load was applied by the vertical actuator.

2.5 Loading program

During the testing, the axial load was kept approximately constant, whereas the lateral force was cycled based on mixed lateral force/displacement control to assess the structural characteristics of the specimens beyond their strength limit. Loading reversals in the push and pull directions were symmetric. Cyclic force was applied to the specimen until the longitudinal bar or angle yielded. Then the loading program was changed to the displacement control. One loading cycle was

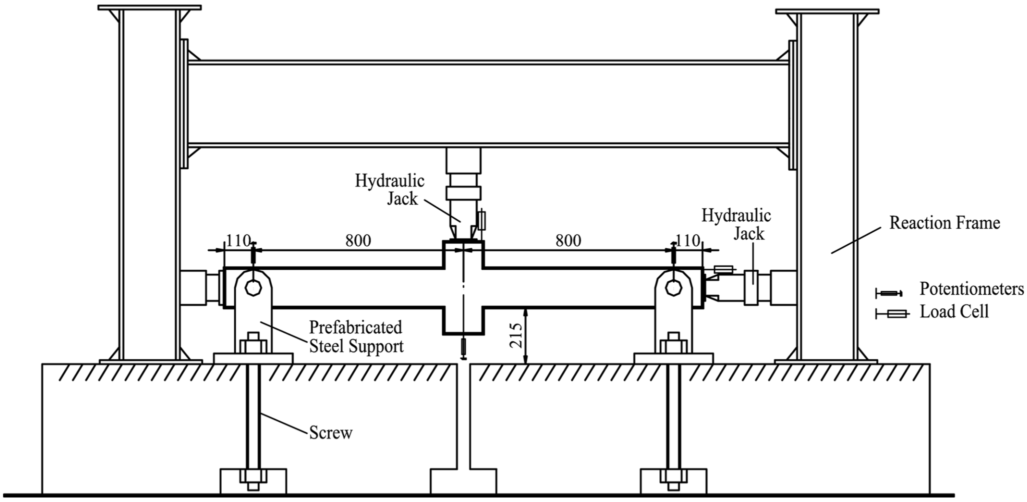

Fig. 2 Test setup

attempted at each displacement amplitude, which approximated to one third of the yield displacement. All specimens were loaded to failure. This was defined as the point at which a sudden loss of load-carrying capacity took place or, in the cases in which this did not happen, as the point at which the load carrying capacity dropped to 85% of the ultimate load.

3. Experimental results

3.1 Observations

The failure behavior for SRC specimens was highly influenced by the level of axial load. The testing axial load ratio n_0, defined as the ratio of the axial force N to the compressive load bearing capacity of the section concrete $f_c bh_0$, is listed in Table 1. The larger the axial force applied, the later cracking appeared. All specimens failed in flexural-shear mode. It was seen that cracks were first observed at the tensile side of the mid-span and then cross cracks appeared diagonally extending from the support to the loading point. Spalling of cover concrete was also observed.

3.2 Hysteresis response

Fig. 3 shows force-displacement loops of the SRC specimens. The hysteresis relations are nearly linear within the first two loading cycles. After concrete cracked, deformation increases more rapidly than lateral force. This denotes that the specimens enter nonlinear range of deformation. The unloading curves within the first several cycles are almost parallel to the loading curve even though they bended a little toward the force axis due to the stiffness degradation of column specimens. With cracks closing at the reverse loading stage, the loading capacities of specimens increase and the loading path almost exceed the peak of the previous hoop. Fig. 4 shows the envelopes of the hysteresis loops and three typical stages can be examined, that are the pre-yield stage, post yield stage, and the softening stage.

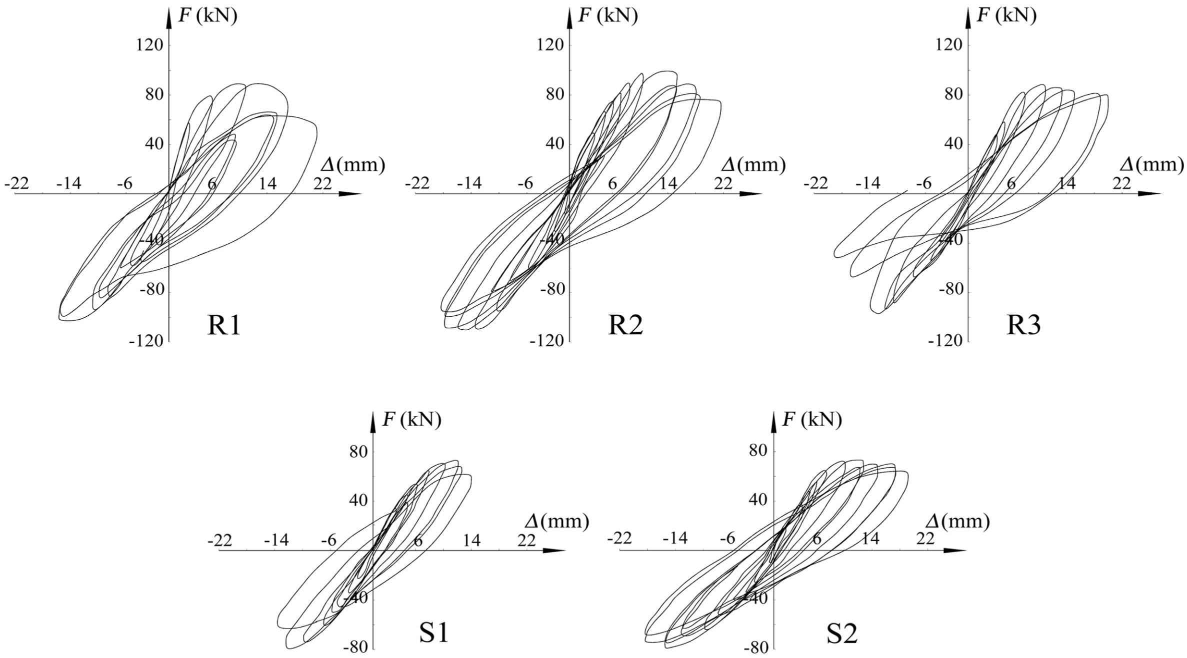

Fig. 3 Response of SRC Columns

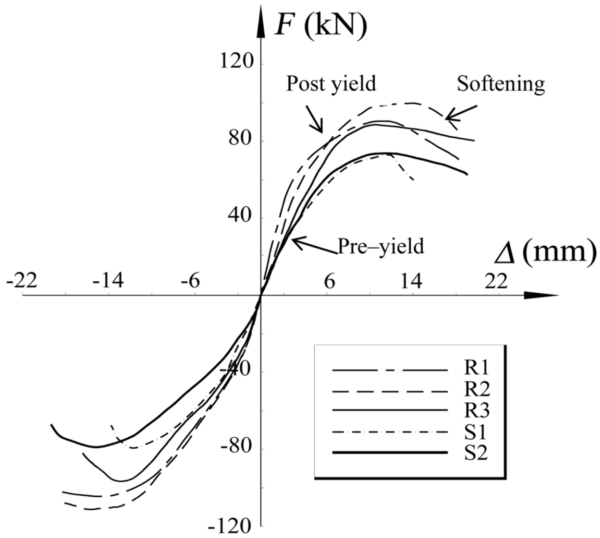

Fig. 4 Envelopes of the hysteresis loops

The examination of testing phenomena and hysteresis response indicate that when loading to failure, SRC specimens behave similarly to RC columns. Hence, the formula of SRC members can be developed based on the mechanism analysis of RC members, which have variety of test data.

4. Modeling of SRC columns

An applied analysis model for structural design and seismic evaluation is generally composed of two typical parts, which are the skeleton curve and the hysteresis rule. The skeleton curve is used to reflect the cracking, yielding and failure characteristics while the hysteresis rule denotes the stiffness degradation, strength deterioration, and pinching effect of the members, as they undergo the reversed cyclic loading in the inelastic range. Usually, key points of the skeleton curve are determined by the theoretical formula and the hysteresis rule is developed from the experimental results.

This paper first builds up the formula of ultimate bearing strength of SRC columns on the basis of the mechanism analysis of RC columns. Then trilinear skeleton curve, normalized by the ultimate strength, is proposed to simulate the envelope curves of the specimens. Theoretical equation of normalizing point (ultimate strength point) was verified by the 5 specimens in this test and 14 SRC columns from parallel tests. Finally, the hysteresis rule characterizing SRC columns is put forward from the experimental loops.

4.1 Skeleton curve

As the ultimate bearing strength point is often more accurate to be determined than the yield point, it is selected here as the basis of modeling normalization. SRC specimens had various ultimate bearing capacities. Normalized by individual ultimate bearing strength and corresponding displacement, experimental envelope curves of the specimens are shown in Fig. 5(a). It can be observed that the nondimensional envelope curves of specimens superpose each other except that at the softening stage they display different declining rate according to their ductility. Thus, normalized envelope curves can be simplified to the trilinear symmetric skeleton curve as shown in Fig. 5(b). In the figure, points Y, U and M indicate the yield point, ultimate strength point and maximum displacement point, respectively, which are also the dividing points of the skeleton curve.

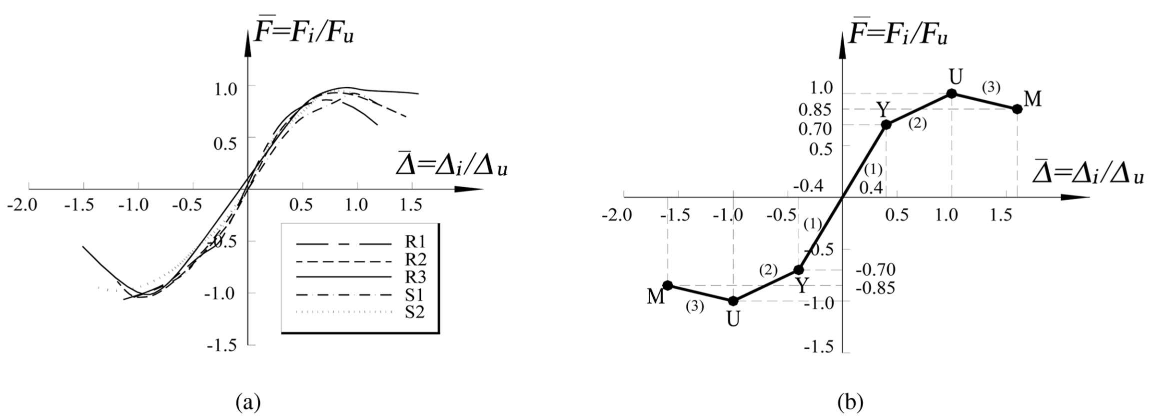

Fig. 5 (a) Normalized envelope curves of the hysteresis hoops, (b) Normalized trilinear skeleton curves of the analytical model

4.1.1 Identification of key point U

Value of ultimate bearing strength

The above-mentioned test of SRC columns shows some correlation with RC columns. The formulation of RC columns can be improved with minor changes to obtain the formulae of SRC columns. The bearing force of RC columns F_u is usually considered based on the following three components equation (Priestley *et al.* 1994, Xiao and Martirossyan 1998).

$$F_u = F_c + F_t + F_a \tag{1}$$

where F_c is the concrete contribution primarily from the concrete aggregate interlock mechanism; F_t is the contribution from the truss mechanism primarily from the lateral reinforcement; and F_a is the arch mechanism contribution and primarily related to the geometry and axial load.

China Academy of Building Research carried out tests of 293 simply supported RC beams only placing the longitudinal bars without hoops (China Academy of Building Research 1994). It was concluded that three physical parameters of the members could reflect the contributions of uncracked compressive concrete and aggregate interlock to the component F_c. They are shear span ratio λ, defined as the ratio of axial distance between the support and loading point to the effective depth of section, compressive strength of the concrete f_c, and ratio of reinforcement of longitudinal bars ρ. The formula obtained from a regression analysis is

$$\frac{F_c}{f_c b h_0} = \frac{0.08}{\lambda - 0.3} + \frac{100\rho}{\lambda f_c} \tag{2}$$

where b = width of section; and h_0 = effective depth of section.

Eq. (2) implies a dependency of F_c on the longitudinal reinforcement ratio. The range of the database was insufficient to determine whether such an influence was significant, and the simplified

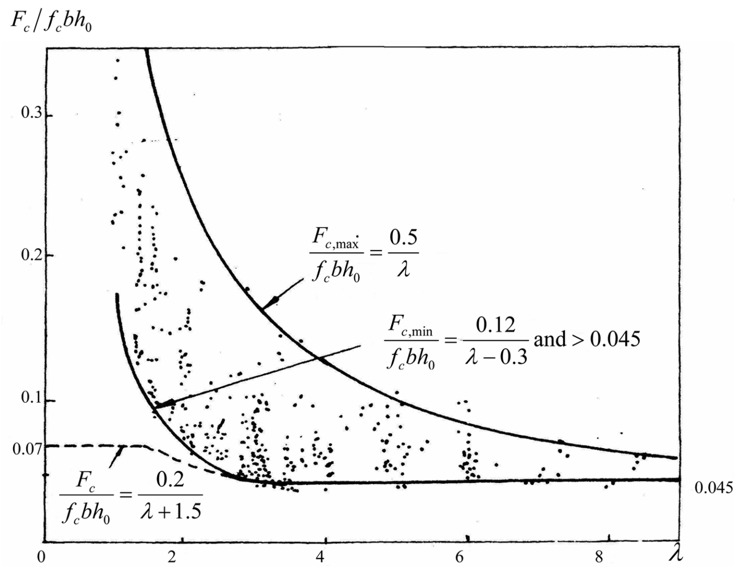

Fig. 6 Upper limit & lower limit of F_c (China Academy of Building Research 1994)

form of Eq. (2) is suggested as below (China Academy of Building Research 1994).

$$\text{Upper limit:} \quad \frac{F_{c,\max}}{f_c b h_0} = \frac{0.5}{\lambda} \tag{3a}$$

$$\text{Lower limit:} \quad \frac{F_{c,\min}}{f_c b h_0} = \frac{0.12}{\lambda - 0.3} \quad \text{and} > 0.045 \tag{3b}$$

The carrying capacity of the concrete columns is taken as the lower limit, as shown in Fig. 6.

$$\frac{V_c}{f_c b h_0} = \frac{0.2}{\lambda + 1.5} \tag{4}$$

where λ should be limited in (1.4, 3.0).

In Eq. (1), F_t denotes the contribution primarily from the lateral reinforcement. According to the truss mechanism, a load-bearing "truss" can be formed by the longitudinal steel angles and bars, lateral hoops and lacings, and inclined concrete between cracks. That is,

$$F_t = 1.25 \cdot \left(f_{sv}\frac{A_{sv}}{s_{sv}}h_0 + f_{av}\frac{A_{av}}{s_{av}}h_0\right) \tag{5a}$$

$$\frac{F_t}{f_c b h_0} = 1.25 \cdot \left(\rho_{sv}\frac{f_{sv}}{f_c} + \rho_{av}\frac{f_{av}}{f_c}\right) \tag{5b}$$

where A_{sv} = total sectional area of stirrups with different legs; s_{sv} = spacing of stirrups along the direction of the member length; f_{sv} = design value of tensile strength of stirrup; ρ_{sv} = ratio of reinforcement of the stirrups; A_{av} = total sectional area of lacings; s_{av}= spacing of lacings along the direction of the member length; f_{av} = design value of tensile strength of lacings; and ρ_{av} = ratio of reinforcement of the stirrups lacings. A parameter of 1.25, as suggested by Priestley for RC columns (Priestley *et al.* 1994), is included in Eq. (5) to consider both the direct bearing capacity and indirect bonded contribution of the lateral reinforcement.

It is considered that compressive axial force enhances the strength by arch action forming an inclined strut. F_a is taken as follows (Code for seismic design of buildings 2001).

$$F_a = 0.07N \tag{6a}$$

$$\frac{F_a}{f_c b h_0} = 0.07\frac{N}{f_c b h_0} = 0.07 n_0 \tag{6b}$$

when axial force $N > 0.5 f_c b h_0$, use $N = 0.5 f_c b h_0$. That is,

$$F_u = \frac{0.2}{\lambda + 1.5} f_c b h_0 + 1.25 \cdot \left(f_{sv}\frac{A_{sv}}{s_{sv}}h_0 + f_{av}\frac{A_{av}}{s_{av}}h_0\right) + 0.07N \tag{7a}$$

$$\frac{F_u}{f_c b h_0} = \frac{0.2}{\lambda + 1.5} + 1.25 \cdot \left(\rho_{sv}\frac{f_{sv}}{f_c} + \rho_{av}\frac{f_{av}}{f_c}\right) + 0.07 n_0 \tag{7b}$$

Data verification by the 5 specimens in this test and 14 SRC columns from parallel tests (Zhou *et al.* 1991, Shi and Bai 2000) is shown in Fig. 7. The formula proposed above is quite accurate to estimate the ultimate bearing strength of SRC columns. Furthermore, force-bearing capacity

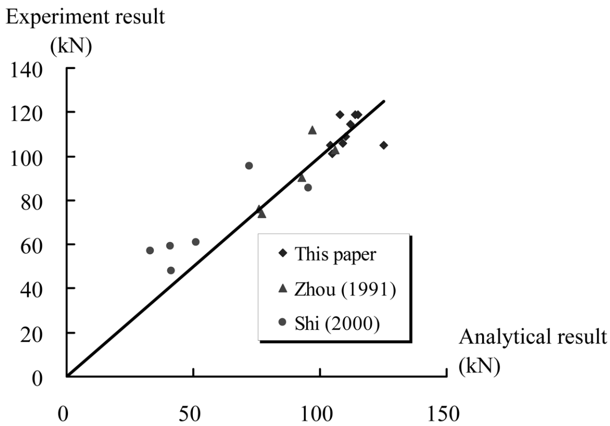

Fig. 7 Formula verification of ultimate bearing strength

increment of angle-shaped steel reinforced concrete columns is mainly attributed to the contribution of steel lacings by adding a term of $f_{av}\frac{A_{av}}{s_{av}}h_0$ to the formula of RC columns.

Deformation corresponding to the ultimate bearing force

A simplified displacement formula corresponding to the ultimate bearing strength is obtained from the parameter analysis of the test, as expressed in Eq. (8).

$$\Delta_u = \frac{2\lambda^2}{\lambda+2}(1.2-n_0)\cdot(0.6\lambda+5\sqrt{\rho_{sv}\cdot\rho_{av}})\cdot L_0/1000 \tag{8}$$

where L_0 = axial length between the support and the loading point.

4.1.2 Identification of key point Y

As shown in Fig. 5(b), the force and displacement of the yield point in the trilinear model are taken to be proportional to those at the ultimate strength point.

$$\frac{F_y}{F_u} = 0.7 \tag{9}$$

$$\frac{\Delta_y}{\Delta_u} = 0.4 \tag{10}$$

4.1.3 Identification of key point M

When the load decreased to 85% of ultimate loading force, the test was terminated and the displacement at that moment was taken as the maximum deformation of the specimens. Parameter μ, so called the displacement ductility factor, is defined as the ratio of the maximum displacement to the yield deformation as formulated in Eq. (11a). Thus, the normalized coordinate of the maximum point is $(0.4\mu, 0.85)$.

$$\mu = \frac{\Delta_{\max}}{\Delta_y} = \frac{\Delta_{\max}}{0.4\Delta_u} \tag{11a}$$

$$\frac{\Delta_{\max}}{\Delta_u} = 0.4\mu \tag{11b}$$

Because the ductility factor of the SRC column decreases under the larger axial force, Eq. (12) was used here to express the relationship between the ductility factor and the axial force ratio.

$$\mu = 2.9 \cdot n_0^{-0.2} \tag{12}$$

As all the key points in Fig. 5(b) have been formulated, normalized trilinear skeleton curve of the applied models of SRC columns are expressed as follows.

$$\begin{aligned}
&(1)\ \bar{\Delta} \le 0.4, \quad \bar{V} = 1.75\bar{\Delta} \\
&(2)\ 0.4 < \bar{\Delta} \le 1.0, \quad \bar{V} = 0.7 + 0.5(\bar{\Delta} - 0.4) \\
&(3)\ 1.0 < \bar{\Delta} \le 0.4 \cdot (2.9n^{-0.2}), \quad \bar{V} = 1.0 - 0.15\frac{\bar{\Delta} - 1.0}{0.4 \cdot (2.9n^{-0.2}) - 1.0}
\end{aligned} \tag{13}$$

where $\bar{V} = F/F_u$, $\bar{\Delta} = \Delta/\Delta_u$. F_u, Δ_u can be calculated from Eq. (7b), Eq. (8), respectively.

Table 3 Experimental results and analytical predictions

Compared parameter \ Specimen name		R1	R2	R3	S1	S2
	Section		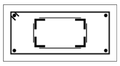		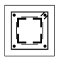	
	n_0	0.69	0.54	0.27	0.73	0.55
Δ_y (mm)	Test	4.6	5.4	5.5	4.4	5.4
	Analysis	4.5	5.7	8.1	4.1	5.7
	(Analysis-Test)/Test	2%	6%	47%	7%	6%
F_y (kN)	Test	63	71	68	56	53
	Analysis	78	72	63	53	52
	(Analysis-Test)/Test	8%	1%	7%	5%	2%
Δ_u (mm)	Test	12.5	15.1	12.4	11.4	13.5
	Analysis	11.1	14.4	20.3	10.2	14.3
	(Analysis-Test)/Test	11%	5%	6%	11%	6%
F_u (kN)	Test	97	106	93	76	77
	Analysis	112	103	90	76	74
	(Analysis-Test)/Test	15%	3%	3%	0%	4%
$\Delta_{\max}$ (mm)	Test	14.6	18.1	21.1	13.8	17.7
	Analysis	13.9	18.8	30.7	12.6	18.6
	(Analysis-Test)/Test	5%	4%	45%	9%	5%
$u = \Delta_{\max}/\Delta_y$	Test	3.2	3.4	3.8	3.1	3.3
	Analysis	3.1	3.3	3.8	3.1	3.3
	(Analysis-Test)/Test	3%	3%	0%	0%	0%

Table 3 shows that most of the typical values calculated by the enhanced formula compared well with those obtained from the experiments. The axial force ratio appreciably effect the analytical displacement. The main reason about the large error of R3 specimen is attributed to some installation and measurement problems in the test.

4.2 Hysteresis rule

In an applied analysis model, hysteresis relation needs to reflect the deterioration of strength, the degradation of stiffness, the pinching effect of the specimens, etc. Observed from Fig. 3, there is no obvious strength deterioration at all and the reloading curve tends to point at the peak point of last loading circle and then go along the skeleton curve.

The experimental unloading stiffness degraded gradually with the increase of the experimental displacement. Based on the data from this test and parallel test (Shi and Bai 2000), the relationship of unloading stiffness to displacement under different axial force in both directions is shown in Fig. 8. It is founded that axial force does not play an important role in the unloading stiffness of SRC specimens. Applied unloading path is selected as straight line here for the reason of model simplicity in the structural design and seismic evaluation. When the effect of the axial force is neglected, the unloading stiffness formula from the fitted regression is expressed as Eq. (14).

$$\overline{K} = 0.8 \cdot (|\overline{\Delta}|)^{-0.3} \tag{14}$$

where $\overline{K} = K/K_0$, K_0 = original stiffness.

It can also be found that at the beginning, the re-loading curve almost directs to a certain fixed point. On the basis of regression analysis, the force of this point is taken as 40% of the load-bearing capacity. There is no obvious pinch effect observed in the load-displacement curves. Thus, fix-point-directed hysteretic constitutive model considering only stiffness degradation has been built up.

The analytical results are compared to the experimentally observed behavior for all SRC column specimens (Fig. 9). It can be found that the simplified model reasonably captures overall the cyclic response. Stiffness degradation and hysteresis shape are quite clearly represented in the analytical results.

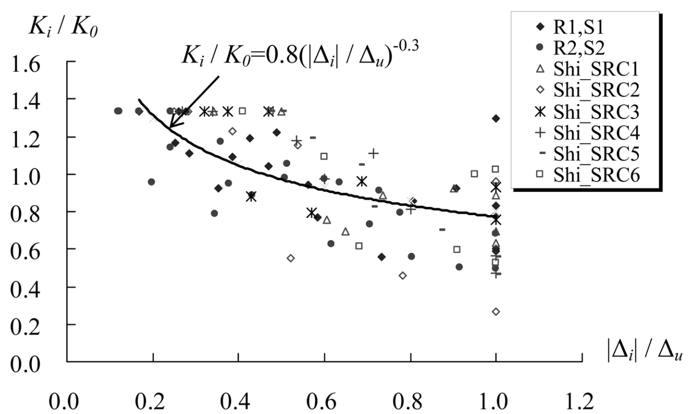

Fig. 8 Normalized unloading stiffness-displacement relationship

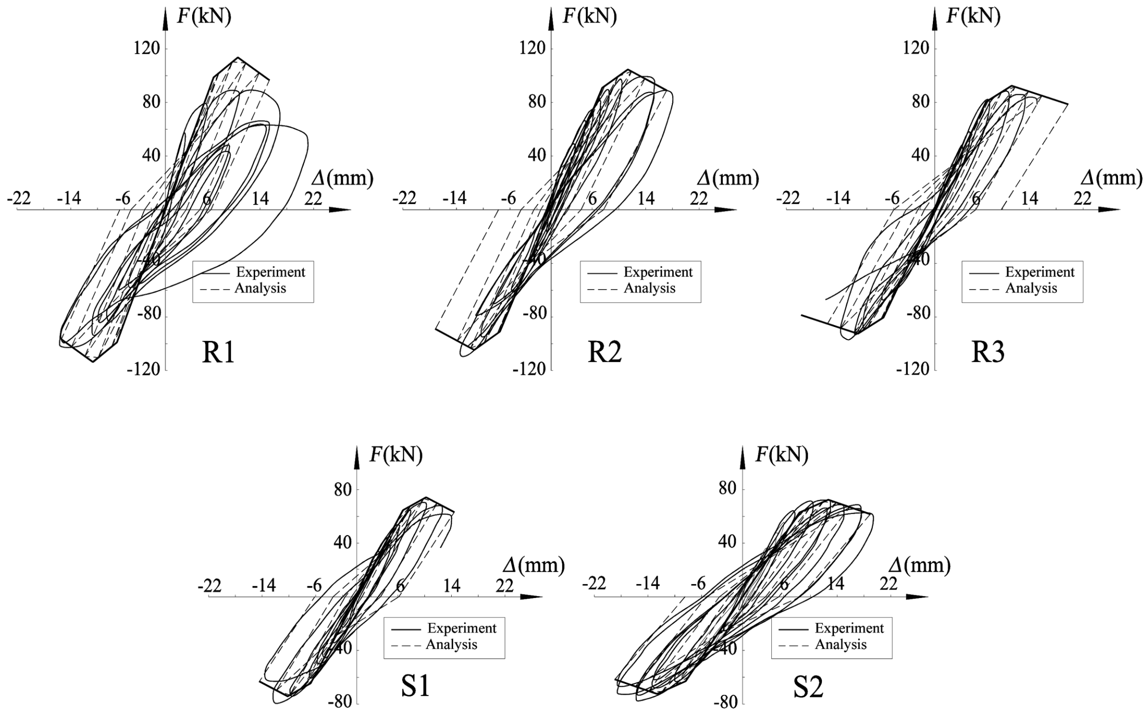

Fig. 9 Analytical and experimental comparison

5. Conclusions

There is a strong feeling within the research and professional community that the future of the structural engineering practice will move towards the increasing use of composite and hybrid structures because these systems provide the benefits for innovation, improved performance, safety, and economy. The following investigations were carried out in this paper.

Firstly, a series of tests of steel reinforced concrete (SRC) columns was described and the test results were analyzed. Secondly an effective analytical approach for the restoring force model of SRC columns was developed for the reliable prediction of the inelastic response of SRC structures. The proposed restoring force model for SRC columns was verified by available test data and it is shown that the simplified model proposed here is effective in capturing the overall load-displacement response of SRC columns. Characteristics of the cyclic response, including stiffness degradation and shape of the hysteresis curve, were clearly represented in the analysis results. However, primary attention should be given to the range of the parameters in this model.

Additional work is focusing on implementing the model to study structural response. As well, the procedure proposed in this paper may be employed in SRC walls to develop simple and applicable model for nonlinear static and dynamic analysis of hybrid wall systems.

Acknowledgements

The authors are grateful for the financial support from the National Natural Science Foundation of

China (Grant 50338040 and 50621062) and Program for Young Excellent Talents at Tongji University.

References

Aschheim M. (2000), "Towards improved models of shear strength degradation in reinforced concrete members", *Struct. Eng. Mech.*, **9**(6), 245-259.
China Academy of Building Research (1994), "No.3 report on reinforced concrete structures", China Architecture & Building Press, Beijing, China. (in Chinese)
Code for Seismic Design of Buildings (GB50011-2001) (2001), China Ministry of Construction, China Architecture & Building Press, Beijing, China. (English Edition).
Deierlein, G.G. and Noguchi, H. (2004), "Overview of U.S.-Japan research on the seismic design of composite reinforced concrete and steel moment frame structures", *J. Struct. Eng.*, **130**(2), 361-367.
El-Tawil, S. and Deierlein, G.G. (1999), "Strength and ductility of concrete encased composite columns", *J. Struct. Eng.*, **125**(9), 1009-1019.
Geol, S. (2004), "United States-Japan cooperative earthquake engineering research program on composite and hybrid structures", *J. Struct. Eng.*, **130**(2), 157-158.
Morino, S. (1997), "Recent developments in hybrid structures in Japan-research, design and construction", *Eng. Struct.*, **20**(2), 336-346.
Park, Y.J., Ang, A.H.S. and Wen, Y.K. (1987), "Damage-limiting aseismic design of building", *Earthq. Spectra.*, **3**(1), 1-26.
Priestley, M.J.N., Verma, R. and Xiao, Y. (1994), "Seismic shear strength of reinforced concrete columns", *J. Struct. Eng.*, **120**(8), 2310-2329.
Ricles, J.M. and Paboojian, S.D. (1994), "Seismic performance of steel-encased composite columns", *J. Struct. Eng.*, **120**(8), 2474-2494.
Shi, J. and Bai, G.L. (2000), "An experimental study on restoring force characteristics of lattice type steel reinforced concrete frame columns", *J. Xian Highway Univ.*, **20**(4), 94-97. (in Chinese)
Spacone, E. and El-Tawil, S. (2004), "Nonlinear analysis of steel–concrete composite structures: State of the art", *J. Struct. Eng.*, **130**(2), 159-168.
Xiao, Y. and Martirossyan, A. (1998), "Seismic performance of high strength concrete columns", *J. Struct. Eng.*, **124**(3), 241-251.
Zhou, Q.J., Jiang, W.S. and Pan, T.H. (1991), "Handbook for hybrid structures", China Architecture & Building Press, Beijing, China, 244-245. (in Chinese)

Notation

The following symbols are used in this paper:
F_u : ultimate bearing strength;
F_c : concrete contribution to the load-bearing capacity;
F_t : contribution of the truss mechanism to the load-bearing capacity;
F_a : arch mechanism contribution to the load-bearing capacity;
λ : shear span ratio;
f_c : compressive strength of the concrete;
ρ : ratio of reinforcement of longitudinal bars;
b : width of section;
h_0 : effective depth of section;
A_{sv} : total sectional area of stirrups with different legs;
s_{sv} : spacing of stirrups along the direction of the member length;
f_{sv} : design value of tensile strength of stirrup;

ρ_{sv} : ratio of reinforcement of the stirrups;
A_{av} : total sectional area of lacings;
s_{av} : spacing of lacings along the direction of the member length;
f_{av} : design value of tensile strength of lacings;
ρ_{av} : ratio of reinforcement of the stirrups lacings;
L_0 : axial length between the support and the loading point;
μ : displacement ductility factor;
K_0 : original stiffness of the specimens;
Δ_u : displacement corresponding to the ultimate bearing strength;
F_y : yield force;
Δ_y : yield displacement;
Δ_{max} : maximum displacement.